Effects of ammonia on combustion, emissions, and performance of the ammonia/diesel dual-fuel compression ignition engine

Nadimi, Ebrahim; Przybyla, Grzegorz; Lewandowski, Michal T.; Adamczyk, Wojciech P.

Link to publication on Research at Birmingham portal

Effects of ammonia on combustion, emissions, and performance of the ammonia/diesel dual-fuel compression ignition engine

Ebrahim Nadimi [a],[*], Grzegorz Przybyła [a], Michał T. Lewandowski [b], Wojciech Adamczyk [a]

[a] *Department of Thermal Engineering, Faculty of Energy and Environmental Engineering, Silesian University of Technology, Gliwice, Poland*
[b] *Department of Energy and Process Engineering, NTNU, Norwegian University of Science and Technology, Trondheim, Norway*

ARTICLE INFO

ABSTRACT

Ammonia is currently receiving more interest as a carbon-free alternative fuel for internal combustion engines (ICE). A promising energy carrier, easy to store and transport, being liquid, and non-carbon-based emissions which make ammonia a green fuel to decarbonize ICE and to reduce greenhouse gas (GHG) emissions. This paper aims to illustrate the impacts of replacing diesel fuel with ammonia in an ammonia/diesel dual fuel engine. Hence, the effects of various ammonia diesel ratios on emissions and engine performance were experimentally investigated. In addition, a developed 1D model is used to analyze the combustion characteristics of ammonia and diesel. Results show 84.2% of input energy can be provided by ammonia meanwhile indicated thermal efficiency (ITE) is increased by increasing the diesel substitution. Moreover, increasing the ammonia energy share (AES) changed the combustion mode from diffusion combustion in pure diesel operation to premixed combustion in dual fuel mode. Therefore, combustion duration and combustion phasing decreased by 6.8*CAD* and 32*CAD*, respectively. Although ammonia significantly reduced CO_2, CO, and particulate matter (PM) emissions, it also increased NO_X emissions and unburned ammonia (14800 ppm). Furthermore, diesel must be replaced with more than 35.9% ammonia to decrease GHG emissions, since ammonia combustion produces N_2O (90 ppm) that offsets the reduction of CO_2.

1. Introduction

Nowadays, internal combustion engines are used mainly for power generation and transportation. Compression ignition (CI) diesel engines, with high load operation and high efficiency, are commonly used in agriculture, heavy-duty, and marine vehicles [1]. However, conventional diesel engines lead to emissions of GHG such as CO_2. The ongoing developments in diesel engines or after-treatment systems are continuously reducing these emissions [2–4]. Yet, using fossil fuels implies inherent emissions of greenhouse gases, in particular, CO_2. The European Union (EU) has introduced strict limitations in the emissions of heavy vehicles [5]. The EU has also committed to reducing GHG emissions to at least 55% by 2030, according to the Paris climate agreement [6], but the long-term objective is to move towards a carbon-free society. Therefore, alternative green fuels, such as ammonia, could be one of the solutions to achieve this goal. Currently, ammonia is receiving more interest among other green fuels such as hydrogen, ethanol, etc. as a renewable carbon-free hydrogen carrier [7].

Ammonia can be easily stored in the liquid phase at ambient temperature and under a pressure of 8 bar. It has 30% more volumetric energy compared to hydrogen [8,9]. However, hydrogen still is used in power generation in other applications [10,11]. As the second most produced chemical in the world, there are well-established infrastructures to produce and transport ammonia, making it a promising sustainable green fuel [12,13]. However, the challenges in using ammonia as fuel in ICE are the high ignition energy and temperature, low flame speed, and low adiabatic flame temperature compared to diesel fuel. Furthermore, the Lower Heat Value (LHV) of ammonia is around 60% lower than diesel fuel. Nevertheless, the sociometric mixture of ammonia/air has almost the same amount of energy compared to the sociometric mixture of diesel/air [14].

Ammonia is used mainly in spark ignition engines (SI) in dual fuel mode by blending with other promoter fuels such as hydrogen, gasoline, etc., or in pure ammonia mode, according to a recent review [15]. However, using pure ammonia in heavy-duty diesel engines requires a high compression ratio (CR) of around 27 and an auto-ignition temperature of 924 K [16]. Rousselle et al. [17] investigated the limitation of applying pure ammonia to the SI engine. Their results show that it is difficult to operate the engine in low load due to the low CR and high

Nomenclature

m	mass, kg		c	cylinder
V	Volume, m^3		BB	blow by
Q_w	Wall heat transfer, W		ex	exhaust
h	Enthalpy, J		u	Internal energy, J
γ	polytropic coefficient		Q_f	Fuel chemical energy, J
h_w	Heat transfer coefficient, $W/(m^2 K)$		α	Crank angle degree, CAD
D	Bore, m		P	Pressure, Pa
			A_w	Surface area, m^2
Abbreviations			T	Temperature, K
ICE	Internal Combustion Engine		CI	Compression Ignition
SI	Spark Ignition		CR	Compensation Ratio
TDC	Top Dead Center		BDC	Bottom Dead Center
BTDC	Before Top Dead Center		ATDC	After Top Dead Center
BBDC	Before Bottom Dead Center		ABDC	After Bottom Dead Center
ITE	Indicated Thermal Efficiency		GHG	Greenhouse gas
IVO	Inlet Valve Opening		IVC	Inlet Valve Closing
EVO	Exhaust Valve Opening		EVC	Inlet Valve Closing
AES	Ammonia Energy Share		MFB	Mass Fraction of Burned
ISFC	Indicated Specific Fuel Consumption		rpm	Revolutions Per Minute
C	Constant		PM	Particulate Matter
COV	Coefficient of Variation		AFR	Air Fuel Ratio
SOI	Start of Injection		SOC	Start of Combustion
			u	unburned
			w	wall
Subscripts			f	fuel
b	burned		sto	Stoichiometry

speed around 2000 rpm due to the low flame speed of ammonia. However, they also mention that the engine can operate under all conditions by adding 10% hydrogen. In a similar work carried out by Lhuilliera et al. [18], they showed that blending ammonia with 20% hydrogen increases the efficiency and power of the SI engine. However, increasing the hydrogen fraction by more than 20% decreased the indicated efficiency due to the high wall heat loss. Ryu et al. [19] studied direct injection of ammonia with port injection of gasoline for the first time. They suggested a new ammonia injection strategy, and their results revealed that a good ammonia injection timing range is between 320 and 370 before TDC. Grannell et al. [20,21] proved that 70% of the gasoline energy can be replaced by ammonia, resulting in knock-free operation under high load. Although they observed a significant increase in N_2O and NO emissions either in lean or rich operations. Generally, N_2O and NO_x emissions increase due to the presence of N in ammonia (NH_3) [22]. Hence, Westlye et al. [23] measured nitrogen-based emissions in the ammonia/hydrogen-fueled SI engine. They also reported that the NO_x emission of the ammonia-fueled SI engine was 4% higher than the conventional SI engine at all the same operating points. Furthermore, the concentration of N_2O was below 60 ppm for different air-fuel ratios.

CI engines are a promising way to utilize ammonia, especially marine engines due to their high CR, which allows using pure ammonia [24,25]. Recently, Imhoff et al. [26] have analyzed the performance of ammonia powertrains on oceangoing vessels to assess the use of ammonia in the marine sector, concluding that ammonia-fueled CI engines are more efficient and easier to implement than others, such as gas turbines. However, ammonia can be used in dual fuel mode in light CI engines for the transportation sector. In dual-fuel diesel engines, ammonia is used with other fuels, e.g., diesel, to overcome the challenges of burning ammonia. In this approach, ammonia is introduced into the intake manifold, and then the pilot dose of diesel or biodiesel is sprayed to supply the minimum energy required to ignite the ammonia-air mixture [27]. The use of ammonia in dual fuel mode in CI engines is presented in Table 1. This table summarizes the main findings of using ammonia with different fuels and the key studied parameters.

According to the above literature review, there is revived interest in the research and development of using ammonia in ICE to reduce greenhouse gas emissions. For that purpose, it is also important to show that ammonia can be produced in a green and carbon-free way. The suitability of ammonia for SI engines has been successfully proven by using H_2 as a combustion promoter [18]. The utilization of ammonia in CI engines still presents notable research gaps. As can be seen from Table 1, researchers only investigated limited ratios of ammonia with other fuels. Ammonia is known for its carbon-free emissions, yet nitrogen oxides are an issue besides nitric oxides (NO) and nitrogen dioxide (NO_2), cumulatively known as NO_x, nitrous oxide N_2O is of particular concern as it can be emitted from ammonia-diesel combustion and has nearly 300 times larger greenhouse effects than CO_2 on the 100-year time scale. Considering the emissions by the greenhouse effect, it can offset the reduction of CO_2. Furthermore, unburned ammonia on itself can be another challenge for dual fuel diesel ammonia engines. In this work, we investigate the impacts of replacing diesel fuel with ammonia to the maximum possible substitution in the CI engine under full loads conditions. Engine performance and emission characteristics are experimentally studied for various ammonia-diesel ratios. Moreover, 1D model is used to calculate the combustion characteristics indicators. Therefore, ignition delay, combustion phasing and duration are determined for different ammonia diesel ratios. Furthermore, unburned ammonia and N_2O emissions are discussed. Finally, CO_2 equivalent GHG emissions are presented to show the effectiveness of ammonia in reducing GHG emissions even with N_2O emission.

2. Experimental methodology

2.1. Experimental setup

All experiments were carried out on a single-cylinder diesel engine. The engine has been retrofitted for ammonia port injection. Table 2 lists the main specifications of the engine. Fig. 1 demonstrates the schematic of the test rig and experimental apparatus. Ammonia was stored at 10

Table 1
Summary of ammonia in dual-fuel CI engines and its effects on performance and emissions from the literature.

Researchers	Year	Fuel	Main studied parameters	Effects of ammonia
M.I. Lamas et al. [28]	2017	NH_3, H_2, diesel	- NH_3 direction injection	- Ammonia decrease more than 70% of NO_x
Lasocki et al. [29]	2019	NH_3, diesel	- Port injection of ammonia to obtain higher loads	- The high amount of NO - Significant reduction of CO_2 and CO
Ryu et al. [30]	2014	Direct injection NH_3, dimethyl ether	− 40% dimethyl ether and 60% NH_3. − 60% dimethyl ether and 40% NH_3	-Suggested injection timing between 90 and 340 BTDC. - Soot and CO decreased. - NO_x and HRR increased
Grosset al. [31]	2013	Direct injection NH_3, dimethyl ether	− 80% dimethyl ether and 20% NH_3 − 60% dimethyl ether and 40% NH_3	- Longer ignition delays. - Combustion temperature decreased. -Increasing injection pressure improved combustion and emissions
Sivasubramaniana et al. [32]	2019	NH_3, mustard methyl ester	- Various loads − 10% and 20% of ammonia	- NO_x reduction of 3.9%. - Combustion temperature decreased. − 10.4% reduction of HC and 3.8% of CO
Wang et al. [33]	2013	H_2, NH_3, diesel	− 10% of H_2	- Increase in NH3 slip, ignition delay, and NO_2. - Efficiency was similar to only diesel operation
Yousefi et al. [34]	2022	NH_3, diesel	- Ammonia energy fraction - Diesel injection timing	−40% of ammonia reduced the NO_x by around 58.8%. - Ammonia emission 4445 ppm
Frost et al. [35]	2021	Aqueous ammonia diesel	- Ammonia diesel load contribution - Different engine loads	- Ignition delay increased. - In-cylinder pressure peak increased. - Significant unburnt ammonia
Yousefi et al. [36]	2022	Ammonia, diesel	-Split diesel injection	- unburned NH_3 decreased 85.5%. - Greenhouse gas emissions decreased 23.7%. - ITE increased 2% by split injection.

Table 1 (*continued*)

Researchers	Year	Fuel	Main studied parameters	Effects of ammonia
lee et al. [37]	2018	Ammonia, diesel	-Injection strategy	- NO is a function of SOI instead of engine load. -NO decreased from 8500 ppm to 3040 ppm by adjusting the SOI.
Nadimi et al. [38]	2022	Ammonia, biodiesel	-Different loads	- Longer ignition delay. - NO emission increased

Table 2
Specifications of diesel engine.

Engine info.	Valves	Units
Engine model	4 stroke, Lifan	
Bore and stroke	86×70	mm
Geometric CR	16.5:1	
Maximum power (3500 rpm)	6.4	kW
Conn. rod length	117.5	mm
IVO	14°	BTDC
IVC	45°	ABDC
EVO	50°	BBDC
EVC	16°	ATDC
SOI	−15.5	BTDC
Injection pressure	200	bar

bar in the cylinder and continuously injected into the intake port at 2 bar. The ammonia mass flow rate was measured with a Coriolis flow meter. A surge tank was installed before the intake manifold to prevent ammonia backflow and to decrease pressure oscillations. The air mass flow rate has been measured using a turbine-type flow meter. The temperatures of the inlet air, the exhaust gas (T_{ex}), diesel fuel, ammonia before injection, and the intake port (T_{port}) were measured. Cylinder pressure traces have been measured using a piezoelectric pressure transducer with a resolution of 1024 measuring points per shaft rotation and for 100 consecutive cycles. An electric motor dynamometer was coupled to the engine to control the engine load and rotational speed. All measured parameters have been monitored with LabVIEW software and National Instruments hardware.

A Fourier Transform Infrared Spectroscopy (FTIR) from Gasmet company (Gasmet DX4000) was used to analyze the exhaust gases. Calcmet software runs FTIR that can analyze 50 gas components in corrosive and wet gas streams at the same time. Various spectrum libraries are embedded in the software that can determine the concentration of each species with an accuracy of 2%. Besides FTIR, an additional gas analyzer is used to verify the measured emissions. Particulate Matter (PM) was measured using SMG200 M with a precision of 3% and particle sizes in the range of 0.04 μm–10 μm under normal conditions (1 atm and 0°C). The exhaust gas sample has been taken directly from the exhaust port through a heated pipe of FTIR at 180 °C.

2.2. Experimental methods

The test was carried out to determine the maximum diesel that can be replaced with ammonia. In addition, the impact of the Ammonia Energy Share (AES, calculated by Eq. (9)) on engine performance, combustion, and emissions characteristics was examined. Since ammonia has a low flame speed and a high minimum required ignition energy [39,40], low engine speed fixed at 1200 rpm and full load were chosen for all operating conditions. The first operating point regarded as the reference was taken at those conditions fueled with pure diesel. Subsequently, the
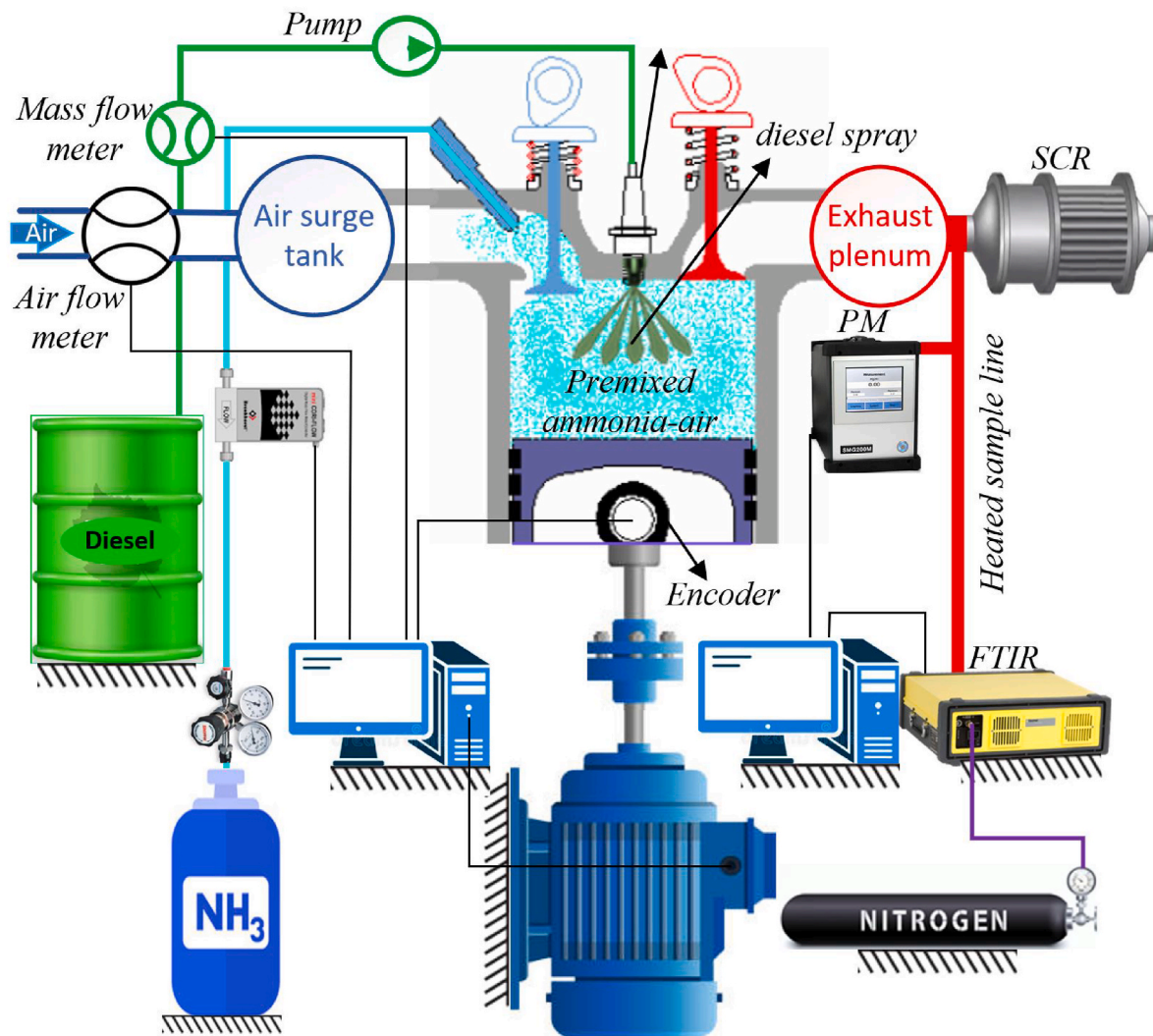
Fig. 1. The schematic of the test rig configuration.

mass flow of diesel is reduced and gaseous ammonia is aspirated to the intake port close to the inlet valve according to the AES values in Table 3, to achieve the same power as in the case of pure diesel.

Introducing more ammonia into the intake manifold to obtain a higher AES, decreases the air mass flow rate. Furthermore, the *LHV* of ammonia is lower compared to that of diesel, which requires a higher mass flow rate to achieve the same power as pure diesel. The stoichiometric air fuel ratio (*AFR$_{sto}$*) of the mixture decreases with increasing ammonia ratio, as ammonia has a stoichiometric AFR of 6.0 [41]. Thus, λ varies between 1.34 and 1.52 for all operating points, as reported in Table 3. The Coefficient Of Variation (COV) for maximum cylinder

pressure (*COV$_{P_{max}}$*), the location of the peak of the in-cylinder pressure and IMEP (*COV$_{IMEP}$*) have been calculated for each test and are presented in Fig. 2. COV is less than 2%, as can be seen in Fig. 2. However, it increases dramatically to 6.0% for maximum AES, which means unstable operation. Therefore, the maximum diesel fuel that could be replaced with ammonia was *AES* = 84.2% and for a higher value of AES, the engine could not run.

Table 3
Overview of the operating points conditions.

| NO.	$\dot{m}_{diesel}$	$\dot{m}_{NH_3}$	$\dot{m}_{air}$	Y_{NH_3}	AES	T_{port}	T_{Ex}	P_i	AFR_{sto}	λ
	g/s	g/s	g/s	–	%	°C	°C	kW	kg/kg	–
OP1	0.220	0	4.27	0	0	33.6	460	3	14.59	1.35
OP2	0.186	0.074	4.25	0.286	14.90	31.3	450.6	3.05	12.15	1.36
OP3	0.152	0.135	4.25	0.470	27.94	28.1	399.2	3	10.58	1.41
OP4	0.127	0.162	4.25	0.561	35.85	26.6	387.7	2.95	9.80	1.51
OP5	0.103	0.212	4.21	0.674	47.44	26.0	373.5	3	8.84	1.52
OP6	0.09	0.249	4.15	0.735	54.81	24.9	370.6	3.06	8.32	1.48
OP7	0.076	0.279	4.03	0.786	61.62	24.8	357.7	3.06	7.89	1.45
OP8	0.040	0.338	3.97	0.894	78.73	23.6	335.4	2.98	6.96	1.51
OP9	0.030	0.364	3.88	0.924	84.16	22.5	328	3.03	6.71	1.47
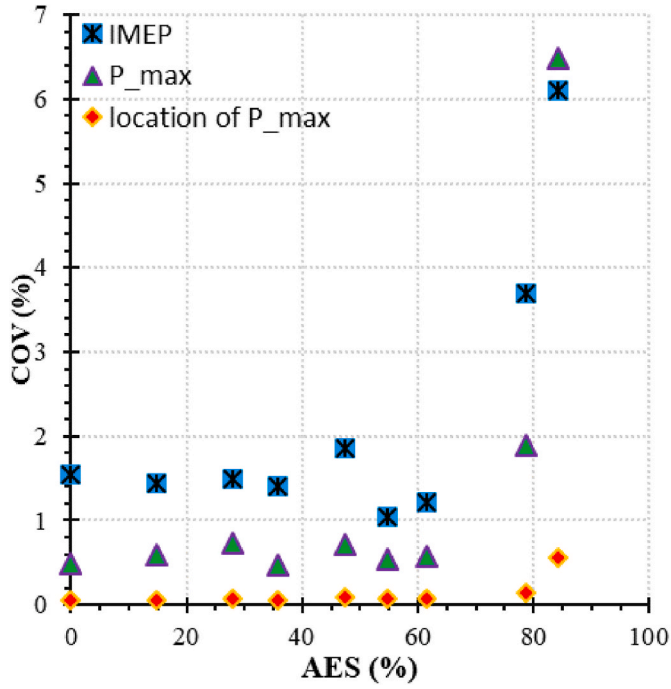
Fig. 2. *COV* of IMEP, the location of the maximum pressure, and peak of the in-cylinder pressure against AES.

3. Numerical methods

3.1. One dimensional model setup

A 1D model was used to analyze the ammonia-fueled engine by using AVL BOOST software and the BURN utility. A method called the "target pressure curve 2 zone" is used to model combustion in the cylinder. In this model, the measured in-cylinder pressure curves are used to calculate the Mass Fraction of Burned (MFB) fuel and the Heat Release Rate (HRR) profiles [42]. Hence, the combustion zone in the cylinder is divided between the unburned and burned gas regions [43]. The first law of thermodynamics is applied to the burned and unburned regions to calculate the gas temperature for each region [44,45]. First law for the burned zone:

$$\frac{dm_b u_b}{d\alpha} = -P_c \frac{dV_b}{d\alpha} + \frac{dQ_F}{d\alpha} - \sum \frac{dQ_{wb}}{d\alpha} + h_u \frac{dm_b}{d\alpha} - h_{BB,b} \frac{dm_{BB,b}}{d\alpha} \quad (1)$$

And for the unburned zone:

$$\frac{dm_u u_u}{d\alpha} = -P_c \frac{dV_u}{d\alpha} - \sum \frac{dQ_{wu}}{d\alpha} - h_u \frac{dm_B}{d\alpha} - h_{BB,u} \frac{dm_{BB,u}}{d\alpha} \quad (2)$$

The terms $\frac{dm_b u_b}{d\alpha}$, $P_c \frac{dV_b}{d\alpha}$, and $\frac{dQ_F}{d\alpha}$ denote the change in internal energy in the cylinder, the work of the piston, and the chemical energy input of the fuel, respectively. Also, $\sum \frac{dQ_{wb}}{d\alpha}$, $h_u \frac{dm_B}{d\alpha}$, and $h_{BB,b} \frac{dm_{BB,b}}{d\alpha}$ are heat losses from the combustion chamber, enthalpy transfer from the unburned zone to the burned zone, and enthalpy blow-by loss in the cylinder which is taken into account and calculated by the BOOST model [42]. In the above equations Eq. (1), and Eq. (2), the volume of the burned and unburned zone is equal to the cylinder volume:

$$V_b + V_u = V_c \quad (3)$$

and the changes of the volume of each zone are equal to the cylinder volume change:

$$\frac{dV_b}{d\alpha} + \frac{dV_u}{d\alpha} = \frac{dV_c}{d\alpha} \quad (4)$$

The volume work is calculated by Refs. [46,47]:

$$\frac{dW}{d\alpha} = P \frac{dV}{d\alpha} \quad (5)$$

The mass of the burned fuel in each CAD is calculated as follows [48, 49]:

$$MFB(\alpha) = \int \frac{dm_{b,f}}{d\alpha} d\alpha \quad (6)$$

heat transfer Q_{wi} to the combustion chamber walls, namely, the cylinder head, piston, and liner, is determined by using the following equation:

$$Q_{wi} = A_{wi} \times h_w \times (T_c - T_{wi}) \quad (7)$$

where A_{wi} is the surface area, T_c is the cylinder temperature, and T_{wi} is the temperature of the respective chamber wall. The heat transfer coefficient (h_w) is calculated using the following Woschni model [50]:

$$h_w = 130 \times D^{-0.2} \cdot P_c^{0.8} \cdot T_c^{-0.53} \cdot \left[C_1 \cdot C_m + C_2 \cdot \frac{V_D \cdot T_{c,1}}{P_{c,1} \cdot V_{c,1}} (P_c - P_{c,o}) \right]^{0.8} \quad (8)$$

3.2. Performance parameters

Performance parameters monitored in the present study are now described and depend on the fuels' properties and their proportions. The *LHV* of diesel was measured and equals 42.4 MJ/kg, and the *LHV* value for ammonia was taken from the literature as 18.6 MJ/kg [51]. Other characteristic properties of the two fuels are shown in Table 4.

In this work, AES is defined as the ratio of the ammonia input energy to the total input energy in the dual fuel model in Eq. (9).

$$AES = \frac{\dot{m}_{NH_3} \times LHV_{NH_3}}{\dot{m}_f LHV_f + \dot{m}_{NH_3} LHV_{NH_3}} \quad (9)$$

The Indicated Thermal Efficiency (ITE) is defined as follows:

$$ITE = \frac{P_i}{\dot{m}_f \times LHV_f + \dot{m}_{NH_3} \times LHV_{NH_3}} \quad (10)$$

where P_i is the indicated power.

The mole fractions of each species were measured every 5 s in 10 min of a steady-state running engine using FTIR. Hence, the standard deviation of 120 measurements of exhaust gas samples was calculated and added to the figures [38]. Because the composition of the mixture varies for different operating points, the concentration of each species was recalculated according to Eq. (11) in 5% of O_2 [52].

$$(X_i)_{5\%@O_2} = (X_i)_m \left[\frac{20.9\% - 5\%}{20.9\% - (O_2)_m} \right] \quad (11)$$

Where $(X_i)_m$ and $(O_2)_m$ are measured mole fraction of each species and the mole fraction of O_2, respectively.

The indicated equivalent specific fuel consumption is defined in Eq. (12) in the dual fuel engine [53].

$$ISFC_{eq} = \frac{\dot{m}_f + \dot{m}_{NH_3} \frac{LHV_{NH_3}}{LHV_f}}{P_i} \quad (12)$$

4. Results

4.1. Engine performance

The engine was operated to obtain the same power at full load using

Table 4
Fuels elementary analysis and *LHV*.

Fuel	C(kg/kg)	H(kg/kg)	N(kg/kg)	LHV (MJ/kg)
Diesel	0.8078	0.1556	0.0003	42.4
Ammonia	0	0.176	0.824	18.6 [51]

different ammonia-diesel input energy ratios. However, the indicated thermal efficiency varies for various ammonia energy shares. Hence, Fig. 3 shows the increase in ITE with increasing AES. For example, ITE increases from 32.0% for pure diesel operation (OP1) to 37.6% for the maximum ammonia energy share (OP9). This 5.6% point rise in ITE is due to two main reasons. First, during ammonia/diesel combustion the in-cylinder temperature is lower than during pure diesel combustion [31], hence heat losses through the cylinder walls are lower (see eq. (8)). As can be seen in Fig. 4, a higher fraction of ammonia energy reduces the total heat loss through the piston, liner, cylinder, and head walls from 320 J/cycle for the pure diesel operation to 240 J/cycle for the highest AES, while volume work is the same. Secondly, as presented in Fig. 5 exhaust gas temperature decreases with higher AES, thus less energy is brought away. The lowest exhaust gas temperature was obtained at AES = 84.2% which is 132 °C lower than for pure diesel operation. This decrease in exhaust gas temperature is related to the lower in-cylinder temperature of ammonia/diesel combustion in the expansion stroke.

The effects of ammonia (AES) on the equivalent $ISFC_{eq}$ are presented in Fig. 6. $ISFC_{eq}$ decreases as more diesel fuel is replaced by ammonia; for example, $ISFC_{eq}$ decreased from 264g/kWh for the pure diesel mode to 224.9g/kWh for the highest AES. This 14.7% decrease in $ISFC_{eq}$ is related to the higher ITE of the ammonia/diesel operation. A similar trend was reported by Reiter et al. [54].

It is also interesting to assess the financial cost of indicated power P_i by comparing pure diesel operation (OP1) with the ammonia dual fuel mode (OP9). During the pure diesel operation (OP1) the fuel consumption is 264 g/kWh, whereas during the dual fuel operation, the engine consumes 35.6g/kWh diesel and 432.6g/kWh ammonia. Although ammonia consumption is higher, the P_i cost is significantly lower compared to the pure diesel mode. As can be seen in Table 5, the cost of P_i in the ammonia/diesel engine is approximately 0.24€/kWh, which is 44% less than the conventional diesel engine.

4.2. In-cylinder pressure

Fig. 7 shows the effects of ammonia on in-cylinder pressure traces. Increasing the ammonia energy share up to 61.6% increases the peak of
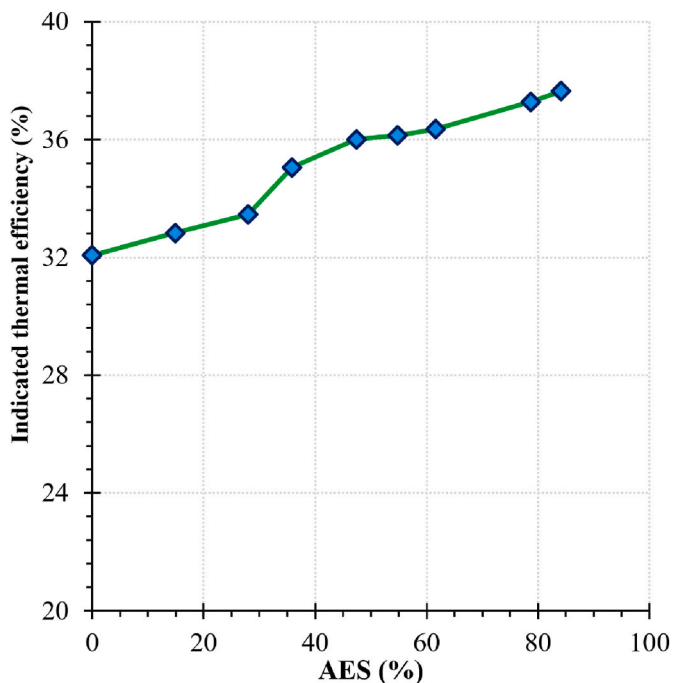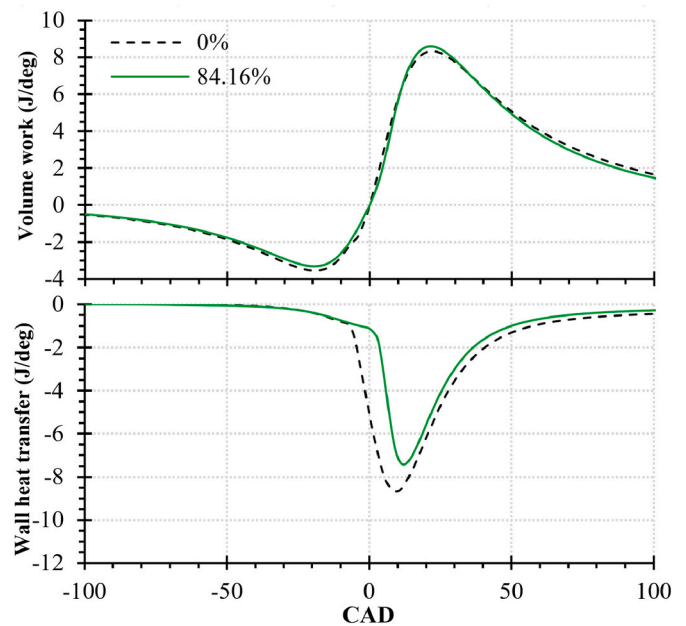
Fig. 4. Volume work and heat transfer of the ammonia/diesel-fueled engine against AES.
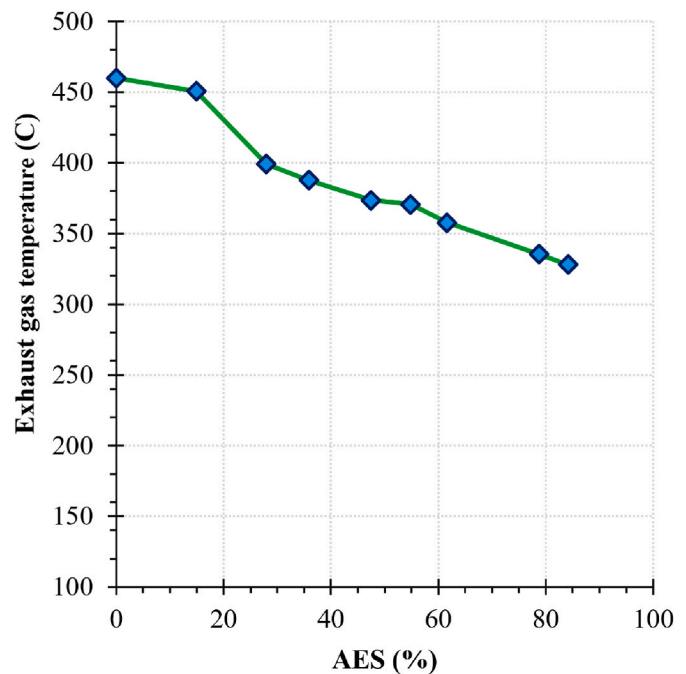
Fig. 5. Effects of ammonia energy share on exhaust gas temperature.

in-cylinder pressure. However for higher AES of 78.7% and 84.2% the peak pressure decreases. Hence, the peak of in-cylinder pressure increases from 76.3 bar for pure diesel to 86.2 bar when the AES is 61.6%. It is related to the fact that combustion occurs a few CAD before the TDC, as can be seen in the Fig. 8 where the maximum Pressure Rise Rate (PRR) is located close to 0 CAD. However, if diesel fuel is replaced with more than 61.6% ammonia, the in-cylinder pressure decreases dramatically since ammonia/diesel combustion occurs after TDC. For example, the pressure drops to 72.7 bar for the highest possible ammonia energy fraction. Furthermore, ammonia has a lower polytropic coefficient (γ) than air [55]. Hence, as more ammonia is introduced into the intake port, the γ of the mixture reduces, and therefore the motored pressure

Fig. 3. Indicated efficiency of the ammonia/diesel fueled engine for different ammonia energy share.
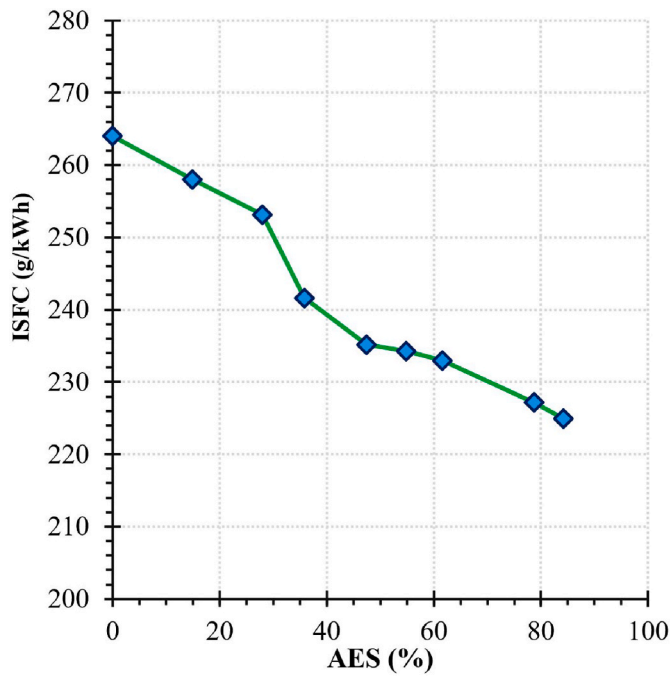
Fig. 6. Equivalent indicated specific fuel consumption of the ammonia/diesel fueled engine.

Table 5
Comparison of P_i cost in the ammonia diesel dual fuel mode with only diesel operation.

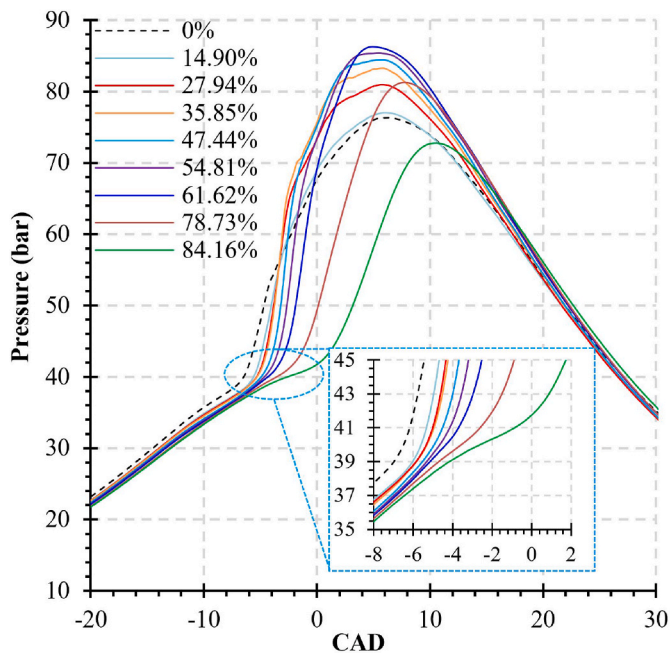| AES	0%	84.16% (dual fuel)	
Fuel	Diesel	Ammonia	Diesel
Fuel price (€/kg)	1.65	0.43	1.65
ISFC (g/kWh)	264	432.67	35.64
P_i cost (€/kWh)	0.43	0.24	

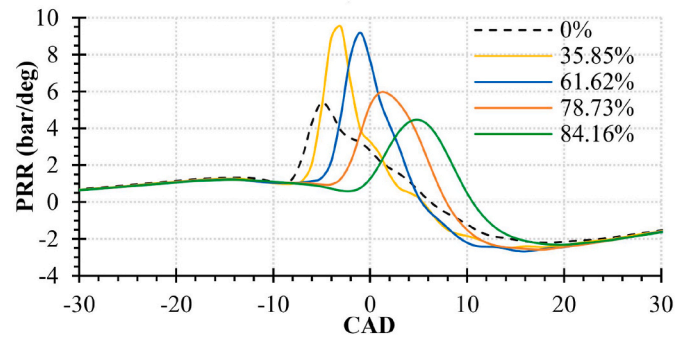**Fig. 7.** In-cylinder pressure traces for different ammonia/diesel ratios.

Fig. 8. Effects of different ammonia diesel energy shares on pressure rise rate traces.

decreases accordingly, as can be seen in Fig. 7. Although the pressure during compression and expansion is low for the highest ammonia energy share, the volume work for pure diesel operation and the AES of 84.2% are the same (Fig. 4).

The first derivative of the in-cylinder pressure known as the pressure rise rate is shown in Fig. 8. The results reveal the delay in the PRR profiles as more diesel is substituted by ammonia, which is caused by the high minimum ignition energy of ammonia compared to diesel. The maximum PRR rises to 9.5 bar/*deg* for the AES of 61.6%, which is 76.5% higher than for pure diesel. Moreover, PRR decreases parabolically for ammonia diesel combustion, whereas it is a linear decline for pure diesel mode. This is due to the combustion of the homogeneous mixture of ammonia air, the short combustion duration, and combustion phasing period. The peak of PRR diagram decreases for the highest AES because combustion starts after TDC (SOC = 0.38*CAD*).

4.3. Effects of ammonia on combustion characteristics

HRR curve of the regular diesel engine typically consists of four phases: ignition delay, premixed combustion, diffusion combustion, and late combustion [56]. However, the HRR diagram for the ammonia/diesel dual fuel mode differs because of the high premixed ammonia-air ratio. Therefore, increasing the ammonia ratio reduces diffusion and the late combustion stage but increases ignition delay and premixed combustion phases, as shown in Fig. 9(a). The HRR curves' peak reveals that high heat was released during the premixed combustion stage. MFB diagram describes the process of chemical energy release and energy conversion as a function of the crank angle. In addition, the characteristics of the combustion phases are determined by the MFB curves, such as the duration of combustion and the ignition delay (Fig. 13) [57,58]. The impacts of AES on the mass fraction of the burned ammonia/diesel mixture are presented in Fig. 9(b). The exponential growth of the MFB curves with increasing AES indicates premixed combustion as a result of the perfect mixing of ammonia and air. Hence, a shorter MFB can enhance output work during the combustion process [59].

Ammonia is known for its low flame speed and high ignition delay time. A pilot fuel is needed to provide the ignition energy to initiate combustion of the premixed ammonia-air mixture. The start of combustion and flame initiation are shown in Fig. 10(a). As more diesel is replaced with ammonia, SOC, CA05, and CA10 are delayed. However, for AES between 0 and 35.85%, the SOC and the ignition delay do not change. The ignition delay is almost 8 CAD when the AES is less than 35.9% due to the higher portion of diesel fuel. Fig. 10(b) shows that the effective in-cylinder ignition delay time increases from 8.7 CAD in case of pure diesel to 15.9 CAD for the highest AES. This is mainly due to the decrease in air mass flow as gaseous ammonia is introduced into the intake manifold, which decreases the oxygen concentration in the cylinder. In addition, ammonia reduces the compression pressure and consequently in-cylinder temperature; therefore, some of the preignition energy will be used to increase in-cylinder pressure and temperature.
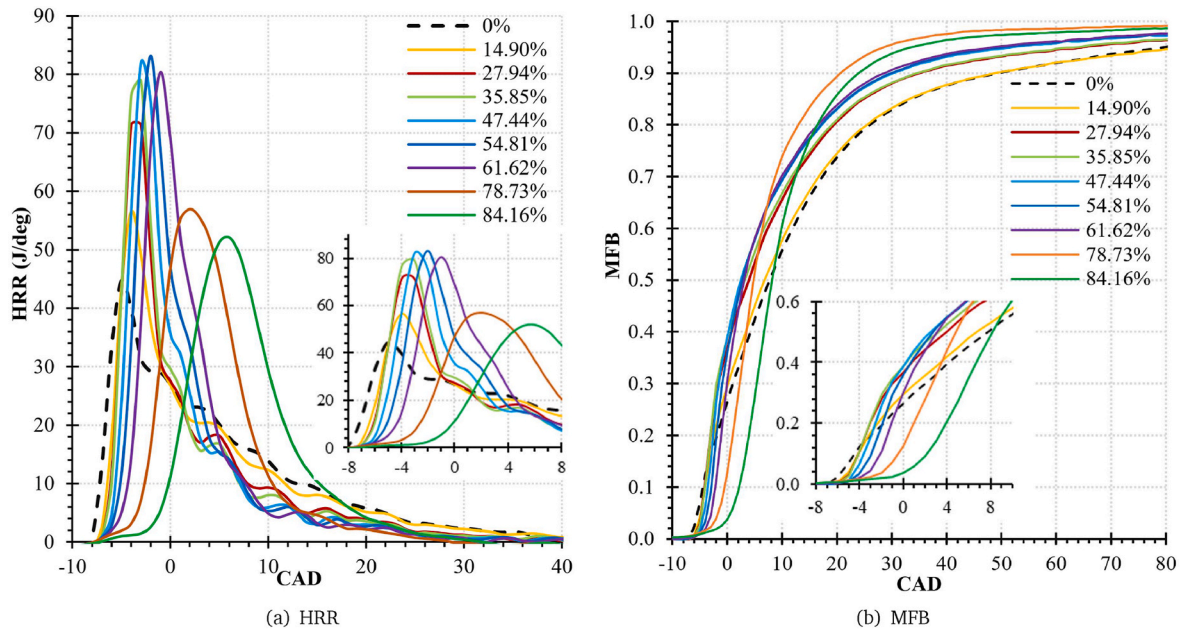
(a) HRR

(b) MFB

Fig. 9. MFB and HRR profiles for different ammonia diesel energy shares.

(a) Start of combustion, CA05, and CA10.

(b) Ignition delay (SOI-SOC), combustion phasing period (SOC-CA50), and location of CA50.
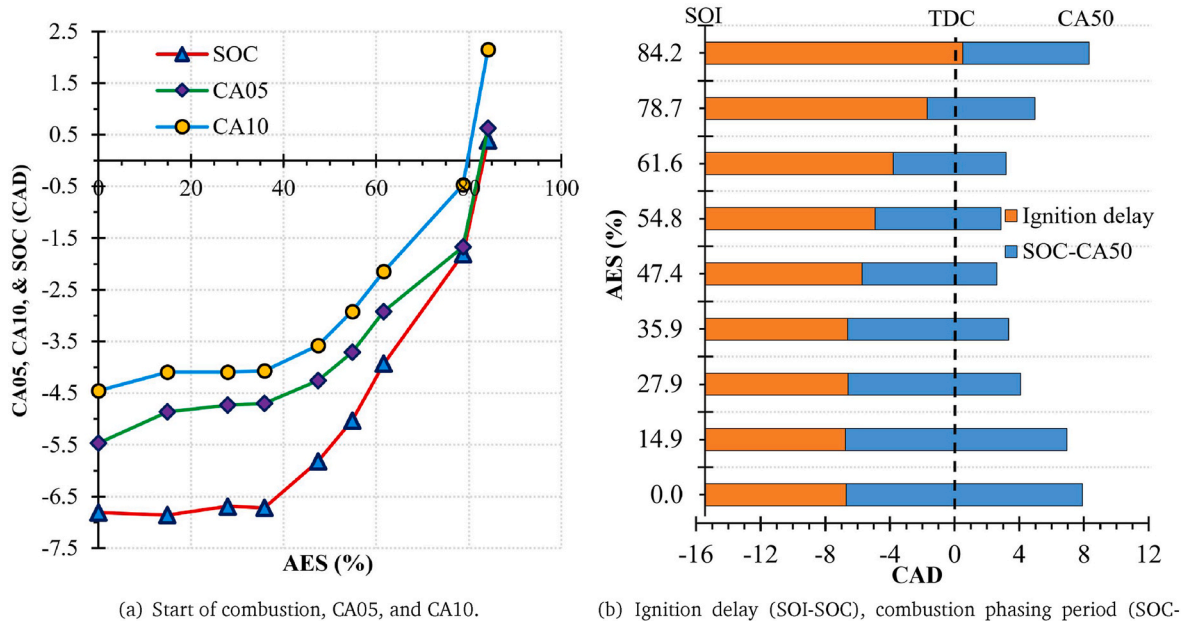
Fig. 10. Ammonia/diesel combustion characteristics indicators for different ammonia energy shares.

Also, ammonia's high required minimum ignition energy and temperature cause this longer ignition delay. For the highest AES, combustion starts in the TDC, where the pressure and temperature are higher as well as there are more desirable thermodynamic conditions for ignition. However, for AES greater than 84.2% combustion does not occur.

Furthermore, the effects of AES on combustion phasing period SOC-CA50 and combustion duration SOC-CA90 are shown in Figs. 10(b) and 11, respectively. As more diesel is replaced by ammonia, the CA50 and the combustion duration are reduced accordingly. Therefore, the CD was reduced from 56 CAD for only diesel operation to 24 CAD for the highest AES. This reduction in CA50 and CD is mainly due to the rapid combustion of premixed ammonia air and the greater heat released during the premixed combustion phase in the HRR diagram compared to pure diesel combustion, as discussed above. Moreover, a higher AES

decreases diffusion and the late combustion phases, resulting in a shorter SOC-CA50 and CD. Tay et al. [60,61] also reported similar results that ammonia decreases the CA50 and combustion duration.

4.4. Emissions analysis

Fig. 12 shows the effects of replacing diesel fuel with ammonia on CO_2 emission and H_2O in the same operation and the indicated power. This figure well demonstrates that ammonia significantly reduces CO_2 emission and instead produces only H_2O. Therefore, increasing the AES from 0 for only diesel mode to 84.2% for the highest diesel substitution, decreased CO_2 emission from 7.0% to 0.9% (7.3 time reduction). Similarly, H_2O increased significantly from 7.4% to 14.9%. Fig. 13(a) illustrates that CO emissions decreased markedly as more diesel fuel is
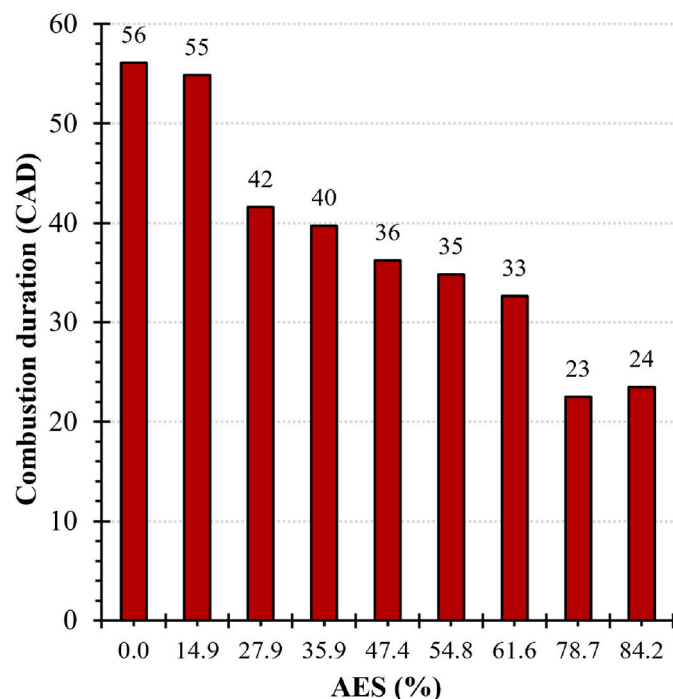
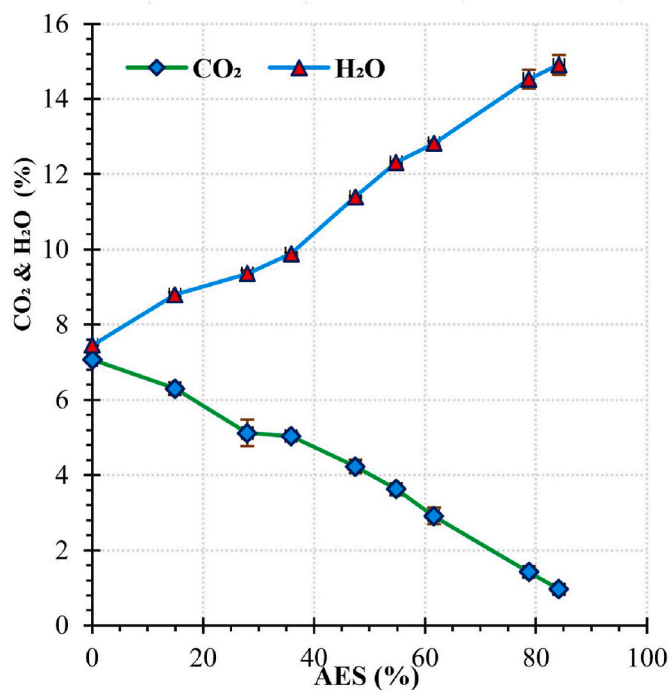**Fig. 11.** Combustion duration (SOC-CA90) of ammonia/diesel fueled engine for various ammonia/diesel ratios.

Fig. 12. CO_2 and H_2O emissions of ammonia fueled diesel engine for various ammonia energy shares.

replaced by ammonia. Hence, *CO* emission decreased drastically from 7592 ppm to 140 ppm. This is due to the fact that replacing diesel with ammonia diminished the carbon atom in the mixture, which results in a reduction in carbon-based emissions. However, the high amount of CO in the pure diesel mode is due to the low engine speed and the full load condition.

Fig. 13(b) illustrates an interesting trend in which NO emission first

decreases and then increases as more ammonia is introduced into the intake port. In other words, some amount of ammonia reduces NO emission, which can be seen in other articles [34,54,60]. Hence, NO emission decreased from 831 ppm for the only diesel case to 491 ppm when AES is 14.9%. Moreover, NO emission is lower than that in the case of pure diesel, while AES is below 35.85%. This is mainly due to firstly, ammonia changes combustion to low-temperature combustion as a result of the low flame temperature of ammonia [62]. Thermal NO formation is less when the combustion temperature is lower. Secondly, Mathieu and Petersen [63] by modeling the ammonia reactions mechanism have revealed that reactions 13, 14, and 15 are the three most dominant reactions with a high sensitivity coefficient in premixed ammonia-air combustion. Therefore, when the amount of NH_3 is low, NO reacts with NH_2 radicals, resulting in a reduction in NO levels.

$$NH_3 + M \rightarrow NH_2 + H + M \tag{13}$$

$$NO + NH_2 \rightarrow NNH + OH \tag{14}$$

$$NO + NH_2 \rightarrow H_2O + N_2 \tag{15}$$

However, as more ammonia was introduced into the intake manifold, NO increased considerably to 2359 ppm at the highest diesel replacement. Because NO formation depends both on the presence of N in NH_3 and on the cylinder temperature. Moreover, since the ignition of the premixed ammonia air starts near TDC for higher AES, this promotes the formation of NO.

Fig. 14 shows N_2O and NO_2 against the input energy share of ammonia/diesel. In general, conventional diesel engines fueled by fossil fuels generally produce a negligible amount of N_2O emission [64]. Thus, N_2O emission is about 3 ppm for the only diesel case. However, as soon as ammonia is injected into the intake manifold, the N_2O emission increased dramatically to 90 ppm and then decreased slightly to 42 ppm for high AES. Although the ammonia diesel dual fuel engine produces a low amount of N_2O emission, but it has 298 times GWP effects compared to CO_2 over 100 years. N_2O is formed during the ammonia ignition process and is nearly absent after complete combustion. It is suggested that N_2O emission can be formed during interruption of ignition and combustion e.g. by quenching on the wall. Therefore, proper design of injection strategy using direct injection of both fuels has a huge chance to improve the reduction of N_2O emission.

Fig. 15 shows the concentration of unburned ammonia in the wet exhaust gas for various ammonia energy shares. Ammonia emission increases significantly as more diesel fuel is replaced by ammonia. Unburned ammonia increased from 7 ppm for only the diesel case to the critical concentration of 14800 ppm for maximum AES. This is likely due to the high amount of excess ammonia in the cylinder, which causes significant amount of unburned ammonia since ammonia is injected continuously into the intake port. Also, owing to the low flame speed of ammonia, which causes unsuccessful flame propagation in the crevices volume, which often causes unburned fuel. More research is needed to reduce this level of unburned ammonia, such as direct injection of liquid ammonia, varying its injection timing and exhaust aftertreatment system. Since an ammonia concentration of more than 50 ppm is hazardous to health.

The effects of different ammonia diesel ratios on particulate matter emission are presented in Fig. 16. It can be observed that increasing the ammonia level significantly reduced the PM emission. In general, soot emissions are promoted by fuel-rich zones and are formed in crevices volume. When the premixed ignition fails in fuel-rich areas, the oxidation can not be complete because of insufficient oxygen. This causes a high PM emission for only diesel operation around 22 mg/m³. However, injecting gaseous ammonia by premixed combustion and reducing the amount of carbon in the mixture decreases PM formation. Therefore, the lowest PM of 4.7 mg/m³ was observed at the maximum AES.
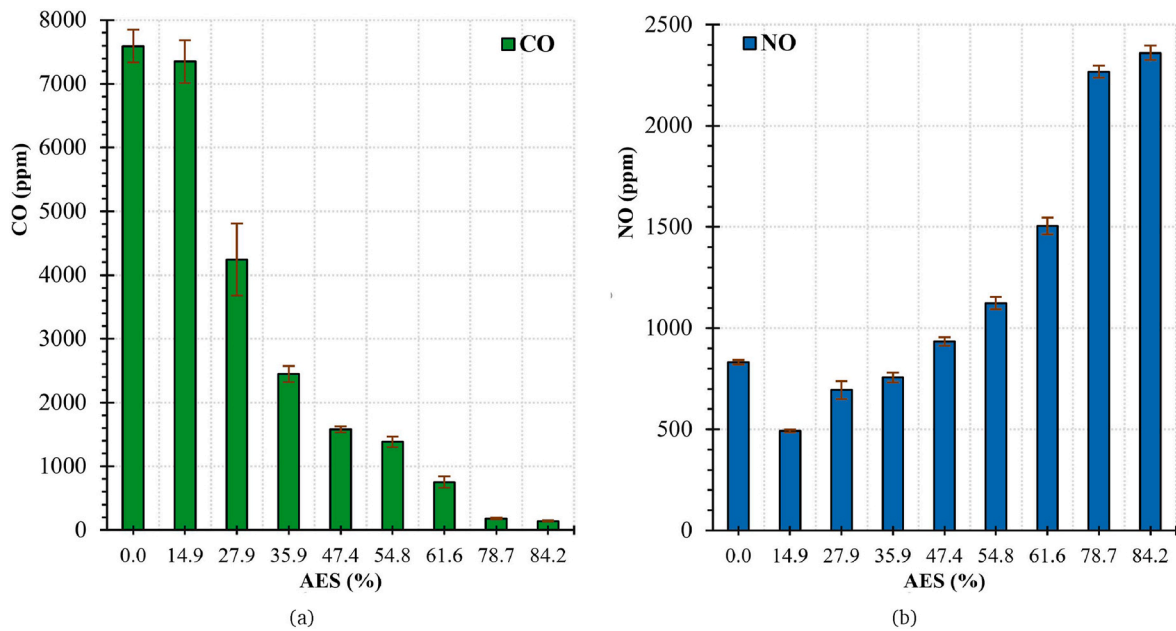
Fig. 13. Effects of ammonia on (a) CO and (b) NO emissions in the ammonia fueled diesel engine.
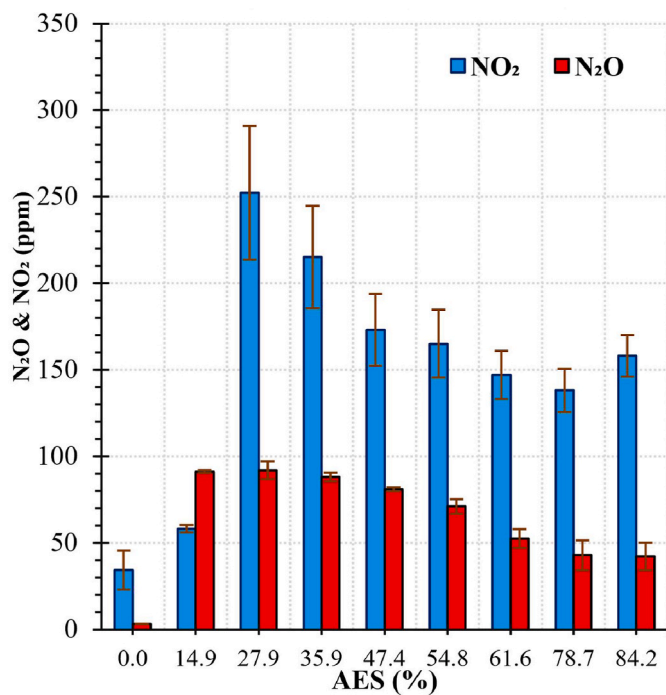

Fig. 14. NO_2 and N_2O emissions in the ammonia dual fuel diesel engine.

Fig. 15. Unburnt ammonia for various ammonia/diesel ratios in the ammonia fueled diesel engine.

4.5. Greenhouse gas emissions and CO_2 equivalents

Ammonia is considered a potential carbon-free fuel for ICE that can reduce CO_2 emissions. Hence, Ammonia diesel dual-fuel engine decreased CO_2 emission by 600g/kWh compared to the conventional diesel engine at the same power and at the highest diesel substitution. However, ammonia combustion in dual fuel mode also produces N_2O emission, which is one of the challenges of ammonia-fueled engines. N_2O is recognized to have a high global warming potential (GWP) of 298 on a 100-year scale relative to CO_2 itself. Therefore, even a small amount of N_2O emission can offset the benefits of reduced CO_2 in the ammonia duel fuel engine. Thus, Fig. 17 shows the GHG emissions for different
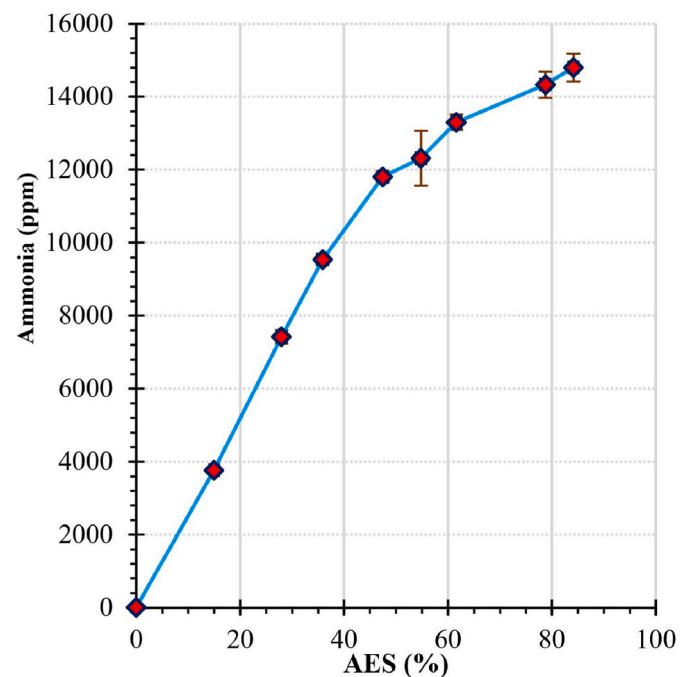
AES. Introducing a small amount of ammonia around 14.9% by input energy significantly increased N_2O emission by 0.84g/kWh (251.9g/kWh of equivalent CO_2) for OP2. This offset the 124.3g/kWh of reduction in CO_2 in OP2. In addition, CH_4 emission is also higher in low AES, which has 28 times GWP relative to CO_2. However, by replacing more diesel with ammonia, CO_2 and therefore total GHG emission decreased significantly. As a result, GHG emissions decreased notably from 727g/kWh for only diesel combustion mode to 243g/kWh for the highest AES. Furthermore, the lower amount of ammonia around 27.9% by AES has higher GHG emissions than the conventional diesel engine.
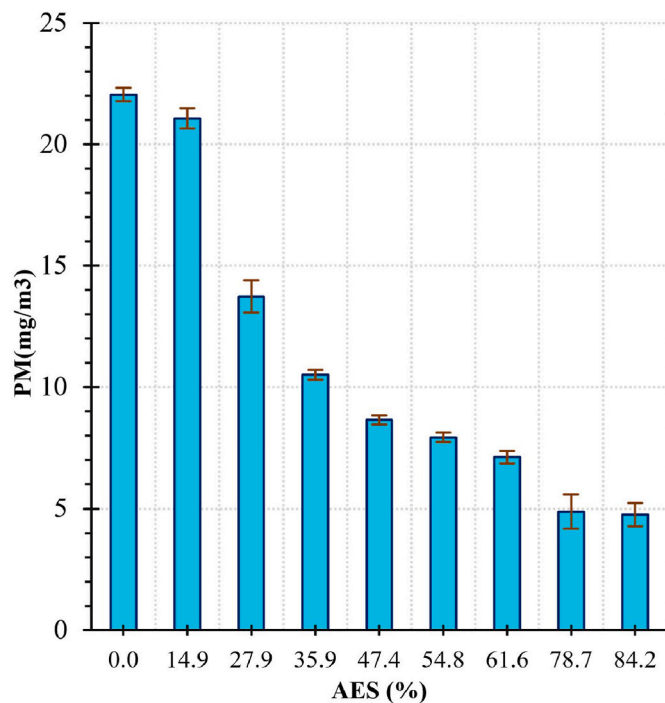
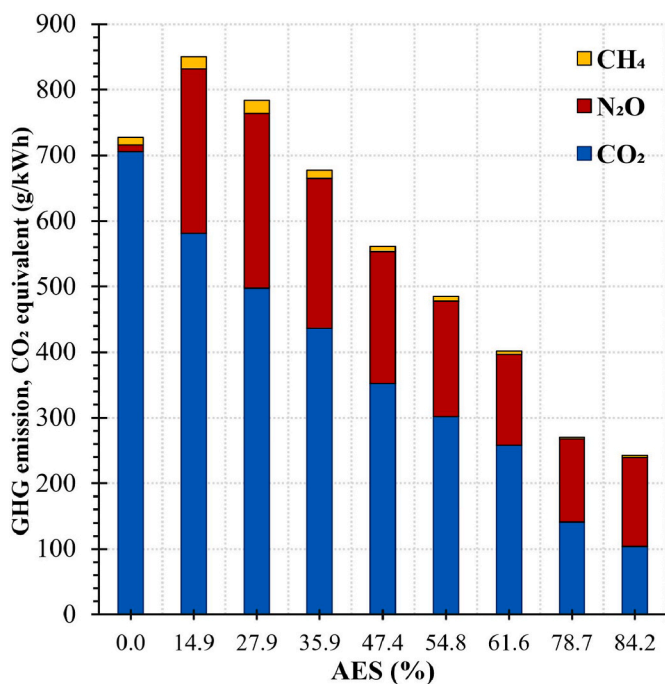**Fig. 16.** Particulate matter emission for different ammonia energy shares.

Fig. 17. Indicated specific GHG emissions equivalent to CO_2 over 100 years for different ammonia/diesel ratios.

5. Summary and conclusions

Ammonia is potential non-carbon fuel to replace current fossil fuels and decarbonize internal combustion engines. An extensive experiment was carried out to study various diesel substitutions with ammonia in the single-cylinder diesel engine. Thus, this work investigates the different ammonia energy shares on ignition, emission characteristics, and engine performance of the ammonia diesel dual fuel CI engine. Moreover, the ammonia/diesel combustion was studied by developed

1D model. The main results of this research are summarized as follows.

- The maximum 84.2% of input energy was provided by ammonia. As more ammonia was introduced into the intake port increased ITE by around 5.6% point at the highest AES. It also reduced the EGT by $132°C$ in this point. The P_i cost of the ammonia/diesel engine is approximately $0.247€/kW.h$, which 43.3% less than the conventional diesel engine.
- Since ammonia has a lower γ than air, the compression pressure decreases by increasing the ammonia mass flow. However, ammonia increases the peak of in-cylinder pressure. Furthermore, it also increases dramatically the peak of PRR to 9.5 bar/deg for AES of 61.6%, which is 76.5% higher than only the diesel case due to premixed combustion.
- Ammonia delayed the SOC by around 7.2CAD at the highest diesel substitution due to the low compression pressure and consequently in-cylinder temperature. Higher ammonia ratio also reduced diffusion combustion phase and increased premixed combustion mode at the highest AES. Thus, the combustion phase and the combustion duration decreased by 6.8CAD and 32CAD, respectively compared to the pure diesel.
- By substituting diesel fuel, carbon-based emissions were markedly reduced, but NO, NO_2 and N_2O emissions increased. However, a significant amount of unburned ammonia was measured that further investigation is need to reduced ammonia emission.
- Ammonia significantly reduced the CO_2 emission from 705g/kWh to 103g/kWh, but it also produced N_2O emission, which has 298 times GHG effects. The GHG emissions decreased when more than 35.9% of diesel was replaced. Hence, the equivalent CO_2 emission of the ammonia dual fuel engine is higher than the case of only diesel when diesel substitution is low. However, GHG emissions decreased significantly from 727g/kWh for only diesel operation to 243g/kWh for the highest AES.

CRediT authorship contribution

Ebrahim Nadimi: Conceptualization, Methodology, Software, Validation, Formal analysis, Investigation, Experiment, Data Curation, Figures, Original draft, Writing - review & editing. **Grzegorz Przybyła:** Conceptualization, Methodology, Investigation, Experiment, Writing - review & editing. **Michal T. Lewandowski:** Writing – review & editing. **Wojciech Adamczyk:** Writing – review & editin, project administration.

Declaration of competing interest

The authors declare that they have no known competing financial interests or personal relationships that could have appeared to influence the work reported in this paper.

Acknowledgment

References

[1] P. Senecal, F. Leach, Diversity in transportation: why a mix of propulsion technologies is the way forward for the future fleet, Results in Engineering 4 (2019), 100060.

[2] S. Khandal, N. Banapurmath, V. Gaitonde, S. Hiremath, Paradigm shift from mechanical direct injection diesel engines to advanced injection strategies of diesel homogeneous charge compression ignition (hcci) engines-a comprehensive review, Renew. Sustain. Energy Rev. 70 (2017) 369–384.

[3] K. Kuta, E. Nadimi, G. Przybyła, Z. Żmudka, W. Adamczyk, Ammonia ci engine aftertreatment systems design and flow simulation, Combustion Engines 61 (2022).

[4] S. Jafarmadar, Multidimensional modeling of the effect of egr (exhaust gas recirculation) mass fraction on exergy terms in an indirect injection diesel engine, Energy 66 (2014) 305–313.

[5] EuropeanCommission, Directive 2015/1513 of the european parliament and of the council amending directive 98/70/ec relating to the quality of petrol and diesel fuels and amending directive 2009/28/ec on the promotion of the use of energy from renewable sources, Off. J. Eur. Union (2015).

[6] G. Liobikienė, M. Butkus, The European Union possibilities to achieve targets of europe 2020 and paris agreement climate policy, Renew. Energy 106 (2017) 298–309.

[7] A. Valera-Medina, F. Amer-Hatem, A. Azad, I. Dedoussi, M. De Joannon, R. Fernandes, P. Glarborg, H. Hashemi, X. He, S. Mashruk, et al., Review on ammonia as a potential fuel: from synthesis to economics, Energy Fuels 35 (9) (2021) 6964–7029.

[8] H. Xiao, S. Lai, A. Valera-Medina, J. Li, J. Liu, H. Fu, Study on counterflow premixed flames using high concentration ammonia mixed with methane, Fuel 275 (2020), 117902.

[9] S. Ni, D. Zhao, Y. You, Y. Huang, B. Wang, Y. Su, Nox emission and energy conversion efficiency studies on ammonia-powered micro-combustor with ring-shaped ribs in fuel-rich combustion, J. Clean. Prod. 320 (2021), 128901.

[10] E. Nadimi, S. Jafarmadar, Thermal and exergy assessment of a micro combustor fueled by premixed hydrogen/air under different sizes: a numerical simulation, J. Appl. Fluid Mech. 13 (4) (2020) 1233–1243.

[11] S. Mohseni, E. Nadimi, S. Jafarmadar, R.A. Rezaei, Enhance the energy and exergy performance of hydrogen combustion by improving the micro-combustor outlet in thermofluidic systems, Int. J. Hydrogen Energy 46 (9) (2021) 6915–6927.

[12] J. Brightling, Ammonia and the fertiliser industry: the development of ammonia at billingham, Johnson Matthey Technology Review 62 (1) (2018) 32–47.

[13] A. Goldmann, F. Dinkelacker, Approximation of laminar flame characteristics on premixed ammonia/hydrogen/nitrogen/air mixtures at elevated temperatures and pressures, Fuel 224 (2018) 366–378.

[14] A.J. Reiter, S.-C. Kong, Demonstration of compression-ignition engine combustion using ammonia in reducing greenhouse gas emissions, Energy Fuels 22 (5) (2008) 2963–2971.

[15] C. Mounaïm-Rousselle, P. Brequigny, Ammonia as fuel for low-carbon spark-ignition engines of tomorrow's passenger cars, Front. Mech. Eng. 6 (2020) 70.

[16] A. Schönborn, Aqueous solution of ammonia as marine fuel, Proc. IME M J. Eng. Marit. Environ. 235 (1) (2021) 142–151.

[17] C. Mounaïm-Rousselle, P. Bréquigny, C. Dumand, S. Houillé, Operating limits for ammonia fuel spark-ignition engine, Energies 14 (14) (2021) 4141.

[18] C. Lhuillier, P. Brequigny, F. Contino, C. Mounaïm-Rousselle, Experimental study on ammonia/hydrogen/air combustion in spark ignition engine conditions, Fuel 269 (2020), 117448.

[19] K. Ryu, G.E. Zacharakis-Jutz, S.-C. Kong, Effects of gaseous ammonia direct injection on performance characteristics of a spark-ignition engine, Appl. Energy 116 (2014) 206–215.

[20] S.M. Grannell, D.N. Assanis, S.V. Bohac, D.E. Gillespie, The fuel mix limits and efficiency of a stoichiometric, ammonia, and gasoline dual fueled spark ignition engine, J. Eng. Gas Turbines Power 130 (4) (2008).

[21] S.M. Grannell, D.N. Assanis, D.E. Gillespie, S.V. Bohac, Exhaust emissions from a stoichiometric, ammonia and gasoline dual fueled spark ignition engine, Internal Combustion Engine Division Spring Technical Conference 43406 (2009) 135–141.

[22] Y. Niki, Y. Nitta, H. Sekiguchi, K. Hirata, Diesel fuel multiple injection effects on emission characteristics of diesel engine mixed ammonia gas into intake air, J. Eng. Gas Turbines Power 141 (6) (2019).

[23] F.R. Westlye, A. Ivarsson, J. Schramm, Experimental investigation of nitrogen based emissions from an ammonia fueled si-engine, Fuel 111 (2013) 239–247.

[24] P. Dimitriou, R. Javaid, A review of ammonia as a compression ignition engine fuel, Int. J. Hydrogen Energy 45 (11) (2020) 7098–7118.

[25] N. De Vries, Safe and Effective Application of Ammonia as a Marine Fuel, 2019.

[26] T.B. Imhoff, S. Gkantonas, E. Mastorakos, Analysing the performance of ammonia powertrains in the marine environment, Energies 14 (21) (2021).

[27] M. Yao, H. Wang, Z. Zheng, Y. Yue, Experimental study of n-butanol additive and multi-injection on hd diesel engine performance and emissions, Fuel 89 (9) (2010) 2191–2201.

[28] M. Lamas, C. Rodriguez, Numerical model to analyze nox reduction by ammonia injection in diesel-hydrogen engines, Int. J. Hydrogen Energy 42 (41) (2017) 26132–26141.

[29] J. Lasocki, M. Bednarski, M. Sikora, Simulation of ammonia combustion in dual-fuel compression-ignition engine, in: IOP Conference Series: Earth and Environmental Science, vol. 214, IOP Publishing, 2019, 012081.

[30] K. Ryu, G.E. Zacharakis-Jutz, S.-C. Kong, Performance enhancement of ammonia-fueled engine by using dissociation catalyst for hydrogen generation, Int. J. Hydrogen Energy 39 (5) (2014) 2390–2398.

[31] C.W. Gross, S.-C. Kong, Performance characteristics of a compression-ignition engine using direct-injection ammonia–dme mixtures, Fuel 103 (2013) 1069–1079.

[32] R. Sivasubramanian, J. Sajin, G. Omanakuttan Pillai, Effect of ammonia to reduce emission from biodiesel fuelled diesel engine, Int. J. Ambient Energy (2019) 1–5.

[33] W. Wang, J.M. Herreros, A. Tsolakis, A.P. York, Ammonia as hydrogen carrier for transportation; investigation of the ammonia exhaust gas fuel reforming, Int. J. Hydrogen Energy 38 (23) (2013) 9907–9917.

[34] A. Yousefi, H. Guo, S. Dev, B. Liko, S. Lafrance, Effects of ammonia energy fraction and diesel injection timing on combustion and emissions of an ammonia/diesel dual-fuel engine, Fuel 314 (2022), 122723.

[35] J. Frost, A. Tall, A.M. Sheriff, A. Schonborn, P. Hellier, An experimental and modelling study of dual fuel aqueous ammonia and diesel combustion in a single cylinder compression ignition engine, Int. J. Hydrogen Energy 46 (71) (2021) 35495–35510.

[36] A. Yousefi, H. Guo, S. Dev, S. Lafrance, B. Liko, A study on split diesel injection on thermal efficiency and emissions of an ammonia/diesel dual-fuel engine, Fuel 316 (2022), 123412.

[37] D. Lee, H.H. Song, Development of combustion strategy for the internal combustion engine fueled by ammonia and its operating characteristics, J. Mech. Sci. Technol. 32 (4) (2018) 1905–1925.

[38] E. Nadimi, G. Przybyla, D. Emberson, T. Lovas, L. Ziolkowski, W. Adamczyk, Effects of using ammonia as a primary fuel on engine performance and emissions in an ammonia/biodiesel dual-fuel ci engine, Int. J. Energy Res. (2022).

[39] S. Frigo, R. Gentili, Analysis of the behaviour of a 4-stroke si engine fuelled with ammonia and hydrogen, Int. J. Hydrogen Energy 38 (3) (2013) 1607–1615.

[40] J.J. MacKenzie, W.H. Avery, Ammonia fuel: the key to hydrogen-based transportation, in: Tech. Rep., Inst. of Electrical and Electronics Engineers, Piscataway, NJ (United States), 1996.

[41] N.J. Vickers, Animal communication: when i'm calling you, will you answer too? Curr. Biol. 27 (14) (2017) R713–R715.

[42] A. Boost, 2-theory, AVL List GmbH, 2013, p. 769.

[43] Ş. Altun, H.F. Öztop, C. Öner, Y. Varol, Exhaust Emissions of Methanol and Ethanol-Unleaded Gasoline Blends in a Spark Ignition Engine, 2013.

[44] G. Noske, A Quasi-Dimensional Model to Describe the Combustion Process in the Gasoline Engine, VDI-Verlag, 1988.

[45] S. Iliev, A comparison of ethanol and methanol blending with gasoline using a 1-d engine model, Procedia Eng. 100 (2015) 1013–1022.

[46] A. Abassi, S. Khalilarya, S. Jafarmadar, The influence of the inlet charge temperature on the second law balance under the various operating engine speeds in di diesel engine, Fuel 89 (9) (2010) 2425–2432.

[47] S. Jafarmadar, M. Mansoury, Exergy analysis of air injection at various loads in a natural aspirated direct injection diesel engine using multidimensional model, Fuel 154 (2015) 123–131.

[48] I. Vibe, Combustion and Cycle Process in Combustion Engines German Translation from Russian by Dr. Joachim Heinrich, 1970 published under the title: Brennverlauf und kreisprozess von verbrennungsmotorenby.

[49] S. Jafarmadar, N. Javani, Exergy analysis of natural gas/dme combustion in homogeneous charge compression ignition engines (hcci) using zero-dimensional model with detailed chemical kinetics mechanism, Int. J. Exergy 15 (3) (2014) 363–381.

[50] G. Woschni, A universally applicable equation for the instantaneous heat transfer coefficient in the internal combustion engine, in: Tech. Rep., SAE Technical paper, 1967.

[51] H. Kobayashi, A. Hayakawa, K.K.A. Somarathne, E.C. Okafor, Science and technology of ammonia combustion, Proc. Combust. Inst. 37 (1) (2019) 109–133.

[52] D.A. Lewandowski, Design of Thermal Oxidation Systems for Volatile Organic Compounds, CRC Press, 2017.

[53] F. Salek, M. Babaie, M.D. Redel-Macias, A. Ghodsi, S.V. Hosseini, A. Nourian, M. L. Burby, A. Zare, The effects of port water injection on spark ignition engine performance and emissions fueled by pure gasoline, e5 and e10, Processes 8 (10) (2020) 1214.

[54] A.J. Reiter, S.-C. Kong, Combustion and emissions characteristics of compression-ignition engine using dual ammonia-diesel fuel, Fuel 90 (1) (2011) 87–97.

[55] Y.A. Cengel, M.A. Boles, M. Kanoğlu, Thermodynamics: an Engineering Approach, vol. 5, McGraw-hill, New York, 2011.

[56] J. Heywood, Internal Combustion Engine Fundamentals, mcgraw-hill book co, New York, 1988.

[57] A. Jamrozik, W. Tutak, M. Pyrc, M. Gruca, M. Kočiško, Study on co-combustion of diesel fuel with oxygenated alcohols in a compression ignition dual-fuel engine, Fuel 221 (2018) 329–345.

[58] K.Z. Mendera, A. Spyra, M. Smereka, Mass fraction burned analysis, J. KONES Internal Combustion Engines 3 (4) (2002) 193–201.

[59] V. Gnanamoorthi, V. Vimalananth, Effect of hydrogen fuel at higher flow rate under dual fuel mode in crdi diesel engine, Int. J. Hydrogen Energy 45 (33) (2020) 16874–16889.

[60] K.L. Tay, W. Yang, J. Li, D. Zhou, W. Yu, F. Zhao, S.K. Chou, B. Mohan, Numerical investigation on the combustion and emissions of a kerosene-diesel fueled compression ignition engine assisted by ammonia fumigation, Appl. Energy 204 (2017) 1476–1488.

[61] K.L. Tay, W. Yang, S.K. Chou, D. Zhou, J. Li, W. Yu, F. Zhao, B. Mohan, Effects of injection timing and pilot fuel on the combustion of a kerosene-diesel/ammonia dual fuel engine: a numerical study, Energy Proc. 105 (2017) 4621–4626.

[62] C. Zamfirescu, I. Dincer, Ammonia as a green fuel and hydrogen source for vehicular applications, Fuel Process. Technol. 90 (5) (2009) 729–737.

[63] O. Mathieu, E.L. Petersen, Experimental and modeling study on the high-temperature oxidation of ammonia and related nox chemistry, Combust. Flame 162 (3) (2015) 554–570.

[64] T. Selleri, A.D. Melas, A. Joshi, D. Manara, A. Perujo, R. Suarez-Bertoa, An overview of lean exhaust denox aftertreatment technologies and nox emission regulations in the European Union, Catalysts 11 (3) (2021) 404.